2019

Detection of Grid Voltage Anomalies via Broadband Subspace Decomposition

Samet Biricik

Soydan Redif

DETECTION OF GRID VOLTAGE ANOMALIES VIA BROADBAND SUBSPACE DECOMPOSITON

Samet Biricik[a,b], *Soydan Redif*[a]

[a] Faculty of Engineering, European University of Lefke, Northern Cyprus,TR-10 Mersin, Turkey
[b] School of Electrical & Electronic Engineering, Dublin Institute of Technology, Ireland

***Abstract*- Due to the increase of sensitive loads on the mains power grid, measurement and monitoring of the power quality (PQ) have become an important factor for both consumers and operators. As is well-known, PQ problems occur in a very short time period with specific characteristics. In transmission or distribution systems, power quality data are collected from monitoring devices such as digital fault recorders, power quality and dynamic system monitors, etc. The recorded data has to be analysed in order to understand system anomalies. These anomalies may be due to sources of broadband noise. In this study, we employ broadband subspace decomposition, using polynomial eigenvalue decomposition, to detect these anomalies. Results demonstrate that this method may be considered as a new and effective tool for measurement and monitoring of PQ problems.**

***Index Terms*—power quality, power system harmonics, PQ monitoring, power distribution, broadband subspace estimation, polynomial EVD, PEVD.**

I. INTRODUCTION

Accurate detection and subsequent eradication of faulty loads connected to the mains grid has received increased attention over recent years. Faulty loads give rise to spurious, intermittent, voltage anomalies on the grid lines. Voltage sags and swells lead to interruption of sensitive loads employed in industry which in turn leads to the significant increase in costs due to loss of production [1],[2]. The analysis of power quality anomalies is a major concern for power systems engineers and designers. Therefore, various methods have been developed to protect equipment and to identify the cause of disturbances. Some of these methods are based on, e.g., the fast Fourier transform (FFT), Kalman filters (KF), decision trees (DTs), fuzzy logic (FL) and neural networks (NNs). One of the most popular methods, in the past, has been wavelet transforms [3]. Reviews of methodologies developed for power quality analysis and power disturbance classification can be found in [4],[5]. The standards refer to methods in the frequency domain for providing a tolerance in the algorithms, such as the Goertzel algorithm, chirp z-transform method, Welch algorithm, zoom FFT, among others, which have all been widely used for electrical-parameter monitoring [6],[7].

However, there are still a number of problems that have not been adequately resolved thus far. A major problem is that some of the voltage anomalies disrupting the grid system occupy a relatively wide band of frequencies, and so should be treated as sources of broadband interference. These types of signal cannot be adequately related in terms of simple phase and amplitude factors across the three-phase utility system. Instead, actual time-delays are required to describe the relationship between the phases. One way of adequately detecting these anomalies is by decorrelating the three phases, which can be performed using matrix factorisation, such as eigenvalue decomposition (EVD). However, using only instantaneous decorrelation would not capture the true relationship between these (broadband) signal phases. Hence, decorrelation over a number of relative time delays, namely strong decorrelation [8], would be more suitable. A matrix of suitably chosen finite impulse response (FIR) filters, or a polynomial matrix [8]-[10], can be applied to the three phase grid voltages to produce strongly decorrelated waveforms. The required polynomial matrix is obtained via a polynomial matrix EVD (PEVD), which has received growing interest recently [10]-[14]. The PEVD has been used to perform convolutive blind source separation and broadband interference rejection in [15]-[18]. In [15]-[17], the PEVD was used to estimate the broadband noise (plus interference) subspace, which then allowed for suppression of the contaminating signals. The second-order sequential best rotation (SBR2) algorithm [10] and its coding-gain variant, SBR2C [11], were used in these works to estimate the PEVD.

In this paper, we proposed a novel method of detecting voltage anomalies in the grid lines, which is based on broadband subspace decomposition. The SBR2C algorithm in [11] is used to estimate the broadband subspace corresponding to the grid anomalies. Our method eliminates the need for pre-processing, such as band-pass filtering, required by most prior-art techniques.

II. PROBLEM DEFINITION

In many cases, consideration of only the instantaneous covariance matrix in characterizing the statistical relationship between the grid-voltage waveforms is not sufficient. This is because the loads that are connected to the grid may corrupt the grid over a significantly large band (broadband) of frequencies; that is, the signals due to the voltage anomalies, such as sag, swell, etc., may consist of a large number of different frequency components. In this case, the broadband signals $\mathbf{x}[t]$ can no longer be related in terms of just phase shifts, since the required phase shift changes with frequency. More appropriately, the relationship between these signals must involve time delays—and/or fractional delays. To adequately describe this relationship a different phase correction is required for each frequency components. This type of operation can be realized by FIR filters, thus

$$\mathbf{x}[t] = \sum_{\tau=0}^{N_A-1} \mathbf{A}[\tau]\mathbf{s}[t-\tau] + \boldsymbol{\eta}[t] \ , \qquad (1)$$

where $\mathbf{A}[t]$ is a 3×3 matrix of FIR filter coefficients $a_{ij}[t] \in \mathbb{R}$, $i,j = 1,2,3$, of order N_A, and $\mathbf{s}[t] \in \mathbb{R}^3$ is the original three-phase grid voltages. In practice, the FIR-filter matrix is unknown. The signal vector $\boldsymbol{\eta}[t]$ denotes the additive white Gaussian noise that is present in the grid lines, which is assumed to be independent from $\mathbf{s}[t]$. Alternatively, this can be expressed using polynomial notation as

$$\boldsymbol{x}(z) = \boldsymbol{A}(z)\boldsymbol{s}(z) + \boldsymbol{\eta}(z) \ , \tag{2}$$

here $\boldsymbol{A}(z) = \sum_{\tau=0}^{N_A-1} \mathbf{A}[\tau]z^{-\tau}$ is a polynomial (or FIR) mixing matrix, or a multi-input, multi-output (MIMO) system, with entries $a_{ij}(z) = \sum_{\tau=0}^{N_A-1} a_{ij}[\tau]z^{-\tau}$, which reflect the frequency-selective nature of the faulty loads attached to the grid; $\boldsymbol{x}(z)$, $\boldsymbol{s}(z)$ and $\boldsymbol{\eta}(z)$ represent vectors of power series with 3×1 coefficient vectors comprising the corrupted, three-phase and noise terms, respectively; for example, $\boldsymbol{x}(z) = \Sigma_\tau \mathbf{x}[\tau]z^{-\tau} = [x_1(z), x_2(z), x_3(z)]^{\mathrm{T}}$.

Due to the filtering in (1) the broadband signals $\mathbf{x}[t]$ will be mutually correlated over a number of time lags, i.e. strongly correlated. Hence, the second-order statistical dependencies between the signals in (1) can be described by the sample space-time covariance matrix [9],[10]:

$$\mathbf{R}[\tau] \triangleq \frac{1}{N}\sum_{t=0}^{N-1} \mathbf{x}[t]\mathbf{x}^{\mathrm{T}}[t-\tau] \ , \tag{3}$$

where τ is a discrete lag parameter, $0 \le t \le N-1$ and $\mathbf{x}[t] = 0$, for $t < 0$ and $t \ge N$. Since $\mathbf{R}[\tau]$ contains auto-covariance, $r_{ii}[\tau] = \sum_\tau x_i[t]x_i[t-\tau]$, and cross-covariance, $r_{ij}[\tau] = \sum_\tau x_i[t]x_j[t-\tau]$, $i \ne j$, functions of $\mathbf{x}[t]$, it follows that $\mathbf{R}[\tau] = \mathbf{R}^{\mathrm{T}}[-\tau]$ [12]. Taking the z-transform of (3) gives the sample cross-spectral density (CSD) matrix of $\mathbf{x}[t]$

$$\boldsymbol{R}(z) = \sum_{\tau=-W}^{W} \mathbf{R}[\tau]z^{-\tau} \ , \tag{4}$$

which is a function of the indeterminate variable z, and has entries $r_{ij}(z) = \Sigma_\tau r_{ij}[\tau]z^{-\tau}$. For the types of broadband signal considered here, the coherence time is significantly small compared to W [10],[17]; therefore, we may assume that $\mathbf{R}[\tau]$ is negligibly small for $|\tau| > W$. Note that, assuming $W \ll N$, an appropriate value for W can be obtained experimentally. The non-diagonal CSD matrix is a parahermitian matrix, that is, it satisfies the parahermitian property: $\boldsymbol{R}(z) = \widetilde{\boldsymbol{R}}(z)$, where $\widetilde{\boldsymbol{R}}(z) = \boldsymbol{R}^{\mathrm{H}}(1/z^*)$ is the parahermitian operation, which involves Hermitian transposition, denoted by the superscript H, and time-reversal, represented by $1/z$. The non-diagonality of the parahermitian CSD matrix $\boldsymbol{R}(z)$ in (4) is indicative of strong correlations between the signals $x_i(z)$ in (2). In many applications, particularly those involving noise suppression, it is important to be able to diagonalize the CSD matrix, which is equivalent to imposing strong decorrelation upon the signals from which $\boldsymbol{R}(z)$ is derived [11]. This can be achieved by calculating the PEVD, or McWhirter decomposition, of $\boldsymbol{R}(z)$, given by [10]:

$$\boldsymbol{R}(z) \approx \boldsymbol{U}(z)\boldsymbol{\Sigma}(z)\widetilde{\boldsymbol{U}}(z) \tag{5}$$

where $\boldsymbol{U}(z)$ is a FIR paraunitary polynomial matrix, which satisfies: $\boldsymbol{U}(z)\widetilde{\boldsymbol{U}}(z) = \widetilde{\boldsymbol{U}}(z)\boldsymbol{U}(z) = \mathbf{I}_3$, where $\mathbf{I}_3$ is the 3×3 identity matrix. The polynomial matrix $\boldsymbol{U}(z)$ may be viewed as an extension of the lossless filter to MIMO systems, the columns of which are the *polynomial eigenvectors* of $\boldsymbol{R}(z)$; and $\boldsymbol{\Sigma}(z) = \mathrm{diag}\{\sigma_{11}(z), \sigma_{22}(z), \sigma_{33}(z)\}$ comprises the estimated *polynomial eigenvalues*, $\sigma_{ii}(z)$, of $\boldsymbol{R}(z)$ – one auto-covariance function for each phase of the grid. Consider application of the FIR paraunitary matrix $\boldsymbol{U}(z)$, from the factorization in (5), to the grid voltages, thus

$$\boldsymbol{v}(z) = \boldsymbol{U}(z)\boldsymbol{x}(z) \ . \tag{6}$$

The transformed signals $\boldsymbol{v}(z) = [v_1(z), v_2(z), v_3(z)]^{\mathrm{T}}$ satisfy strong decorrelation, and are related to the diagonal matrix of polynomial eigenvalues in (5) by:

$$\boldsymbol{\Sigma}[\tau] = \mathcal{E}\{\mathbf{v}[t]\mathbf{v}^{\mathrm{T}}[t-\tau]\} \ , \tag{7}$$

where $(z) = \Sigma_\tau \mathbf{v}[\tau]z^{-\tau}$, $\sigma_{ii}(z) = \Sigma_\tau \sigma_{ii}[\tau]z^{-\tau}$ and $\mathcal{E}\{\cdot\}$ is the expectation operator. Evaluation of the diagonal entries $\sigma_{ii}(z)$ at $z = e^{\mathrm{j}\Omega}$ reveals the power spectral density (PSD) of $v_i[t]$, denoted by $\Sigma_{ii}(e^{\mathrm{j}\Omega})$. It is well-known that $\Sigma_{ii}(e^{\mathrm{j}\Omega})$ satisfy the spectral majorization property [8],[11],[19]:

$$\Sigma_{ii}(e^{\mathrm{j}\Omega}) \ge \Sigma_{i+1,i+1}(e^{\mathrm{j}\Omega}) \ , \tag{8}$$

$i = 1,2,3$, for all normalized frequencies Ω. The spectral majorization property is analogous to the eigenvalue ordering that is performed by an ordered EVD [15]-[17]; and is desirable in a number of applications, including, in particular, broadband interference cancellation [17]. As explained in the next section, this application is highly relevant to the problem of detecting the voltage anomalies embedded in the grid voltage waveforms; where both strong decorrelation and spectral majorization act, in effect, to unravel components of the broadband voltage anomalies from the grid voltages.

The aim of this work, ultimately, is to detect the voltage anomalies on the grid lines. One way of achieving this is through estimates of the broadband noise (plus interference) subspace, which can be obtained from the EVD of $\boldsymbol{R}(z)$ – discussed in Section III. The onset of each voltage anomaly can then be detected using estimates of the voltage anomalies derived from the noise subspace, as described in Sections III.

III. Proposed Method

The spectral majorization property of PEVD algorithms, such as SBR2 [10],[19] and SMD [13], enables their effective use in broadband subspace decomposition, as demonstrated in [15]-[17]. This plays an important role in the proposed approach to detecting voltage anomalies. Our approach can be summarized by the following two steps:

1. Use broadband subspace decomposition via PEVD (SBR2C) to estimate the voltage anomalies.

2. Use peak-detection to identify the onset of the voltage anomalies.

A block diagram of our two-step approach is shown in Fig. 1.

The approximate PEVD in (5) can be used to extend principal component analysis (PCA) to polynomial matrices, or to broadband signals, namely broadband PCA (BPCA) [15]-[17]. Hence, the transformation in (6) can be viewed as the analysis stage of BPCA, where $\boldsymbol{v}(z)$ represent the *polynomial principal components*. This allows extension of the concept of subspace decomposition, or low-rank modelling, to broadband signals, i.e. broadband subspace decomposition [17]. Then the polynomial principal components, which are orthogonal, can be partitioned as:

$$\boldsymbol{v}(z) = \left[\boldsymbol{v}_s(z), \boldsymbol{v}_\eta(z)\right]^{\mathrm{T}} , \tag{9}$$

where $\boldsymbol{v}_s(z)$ defines an estimate of the signal (plus noise) subspace and $\boldsymbol{v}_\eta(z)$ represents the broadband interference and noise subspace. For our application, the former would typically be related to the actual three-phase voltages. This is because the three-phase waveforms are highly correlated with one another—more so than the voltage anomalies would be in general—and so a PEVD algorithm would tend to strongly decorrelate these signals from the noise and interference signals. The noise subspace, on the other hand, would be associated with the voltage anomalies (and noise), since they would typically have weaker correlations than the more prominent three-phase waveforms. For a thorough treatment of broadband subspace estimation in the context of broadband blind source separation the reader is referred to [17],[18].

Assume that the spectra of the voltage anomalies are different from that of the three-phase voltage waveforms. Then estimates of either of the two signals can be obtained by projecting the grid measurements $\boldsymbol{x}(z)$ onto the appropriate broadband subspace. In particular, estimates of the voltage anomalies can be obtained by an orthonormal projection of $\boldsymbol{x}(z)$ onto the noise subspace, represented by $\boldsymbol{v}_\eta(z)$. This can be achieved using the PEVD-designed paraunitary matrix $\boldsymbol{U}(z)$ in a reconstruction or synthesis stage [16],[17]:

$$\boldsymbol{y}(z) = \widetilde{\boldsymbol{U}}(z)\mathbf{B}\boldsymbol{v}(z) = \widetilde{\boldsymbol{U}}(z)\mathbf{B}\big(\boldsymbol{U}(z)\boldsymbol{x}(z)\big) , \tag{10}$$

where $\mathbf{B}$ is a 3×3 matrix that is designed to block principal components related to the pure three-phase signals and $\boldsymbol{y}(z) = [y_1(z), y_2(z), y_3(z)]^{\mathrm{T}}$ contains estimates of the voltage anomalies. Equation (10), as depicted in the highlighted box of Fig. 1, can be viewed as a method for achieving second-order, broadband, blind source separation. However, it should be noted that $\boldsymbol{y}(z)$ are not unmixed signals, in the conventional sense of compensating for the mixing matrix $\boldsymbol{A}(z)$ in (1). The procedure outlined here constitutes broadband subspace decomposition.

The blocking matrix $\mathbf{B}$ takes the form of a null matrix with the exception of strategically placed '1's on its diagonals, the locations of which correspond to $\boldsymbol{v}_\eta(z)$ in $\boldsymbol{v}(z)$. The correct choice of $\mathbf{B}$ depends on our assumptions about the rank of the problem, or the signal-subspace dimension. To estimate the subspace dimension we look at the PSDs of the polynomial eigenvalues, i.e. $\Sigma_{ii}(e^{\mathrm{j}\Omega})$. Due to the spectral majorisation property of (8), an iterative PEVD algorithm, such as SBR2C, will tend to compact the most strongly correlated (pure three-phase) signal-related energies into the first few diagonal elements of $\boldsymbol{\Sigma}(z)$ in (5) [11],[19]. With this assumption in mind, the following routine can be used to make noise-subspace identification an adaptive process:

1. If $\Sigma_{33}(e^{\mathrm{j}\Omega}) \ll \Sigma_{22}(e^{\mathrm{j}\Omega})$, where $\Sigma_{22}(e^{\mathrm{j}\Omega}) \leq \Sigma_{11}(e^{\mathrm{j}\Omega})$, for all Ω, then the noise subspace dimension can be described by the polynomial principal component $v_3(z)$
2. If $\Sigma_{33}(e^{\mathrm{j}\Omega}) \leq \Sigma_{22}(e^{\mathrm{j}\Omega}) \ll \Sigma_{11}(e^{\mathrm{j}\Omega})$, for all Ω, then the noise subspace dimension can be described by the set of polynomial principal components $\{v_2(z), v_3(z)\}$.

An alternative approach would be to make the following assumption. Since $\boldsymbol{\Sigma}(z)$, for the grid system, has only three diagonal elements, it is reasonable to expect $\sigma_{11}(z)$ and $\sigma_{22}(z)$ to be dominant (powerful) diagonal elements, which would be energy related to the pure three-phase signals. The weakest diagonal element, i.e. $\sigma_{33}(z)$, would most likely be related to the voltage anomalies. Assuming this to be true, it is then reasonable to construct $\mathbf{B}$ such that it blocks the first two components of $\boldsymbol{v}(z)$, i.e. $v_1(z)$ and $v_2(z)$. This can be achieved with the following diagonal blocking matrix:

$$\mathbf{B} = \mathrm{diag}\{0,0,1\} . \tag{11}$$

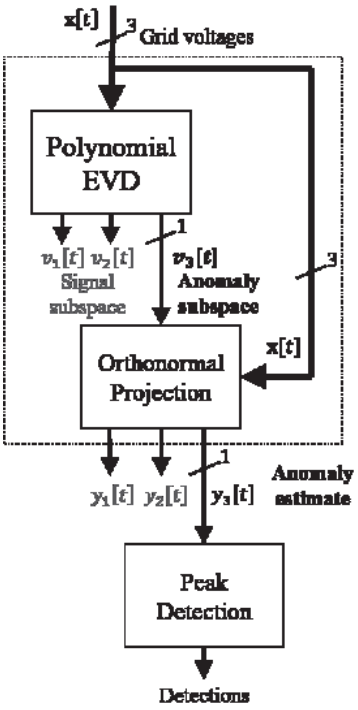

Fig. 1 Block diagram representation of the proposed approach, where the system blocks outlined by the dotted box constitute broadband subspace decomposition.

IV. Experimental Results

To demonstrate the performance of the proposed PQ detection method, we present results from real-time experimentation. In order to observe the performance in a real time environment, the proposed PEVD-based subspace projection method has been verified using the OPAL-RT real-time platform, working under RT-LAB software environment with associated tools, as shown in Fig.2. This system has a total of 16 analogue inputs/outputs and 32 digital inputs/outputs. The system is tested with hardware synchronization mode to obtain real-time communications between the sensing and control signals.

The effectiveness of the proposed method at detecting voltage sags and swells present on the grid lines has been assessed. Figs. 3(a) and 4(a) show the three phases of the grid voltage overlaid on top of each other; phases A, B and C are denoted by the orange, cyan and purple curves, respectively. Fig. 3(a) shows the three-phase voltage sags (from 230 V rms to 150 V rms) that occur on the grid voltage. Fig 3 (b) clearly shows that the faulty interval is detected virtually instantaneously by the proposed algorithm. In Fig 4 (a), we show the case where a voltage swell is applied to the grid voltages – the swell can be observed on all three phases. From Fig 4 (b) we see that the voltage-swell period can be determined accurately using our method. The peak detection algorithm in [20] was used to obtain these results.

V. Conclusion

In this paper, a method for the detection of grid anomalies has been proposed. Our method has been verified experimentally, and the results show that the algorithm detects grid anomalies in an effective manner. Such an algorithm would enable the processing of measured data from PQ monitoring systems, such as digital fault recorders, PQ monitoring devices and dynamic system monitors. A further advantage of the system is that it allows for rapid classification of results. Future work will likely focus on the development of the proposed algorithm for (i) the detection of harmonic distortions; (ii) integration into a digital signal processor for the purpose of controlling power systems devices.

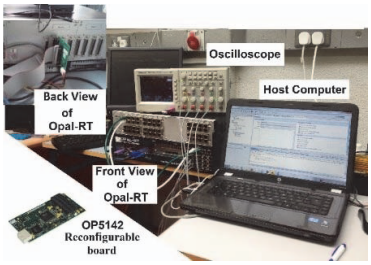

Fig. 2 Real-time laboratory set up with OPAL-RT.

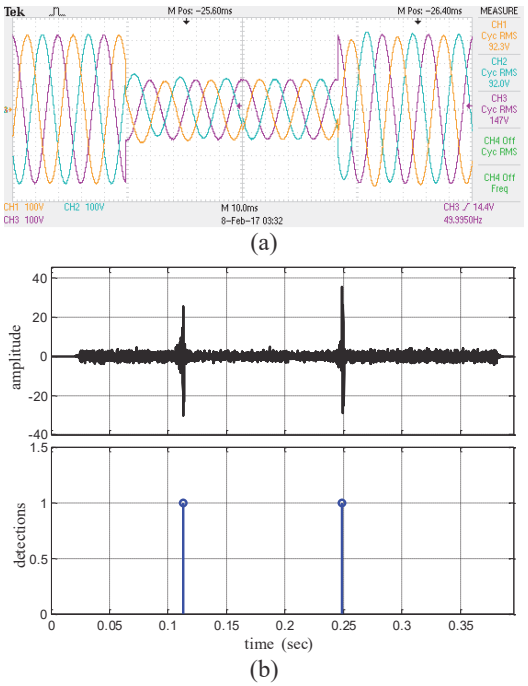

(a)

(b)

Fig. 3 Performance of the proposed system under three-phase voltage sag condition (a) captured results in oscilloscope (b) determined faulty interval.

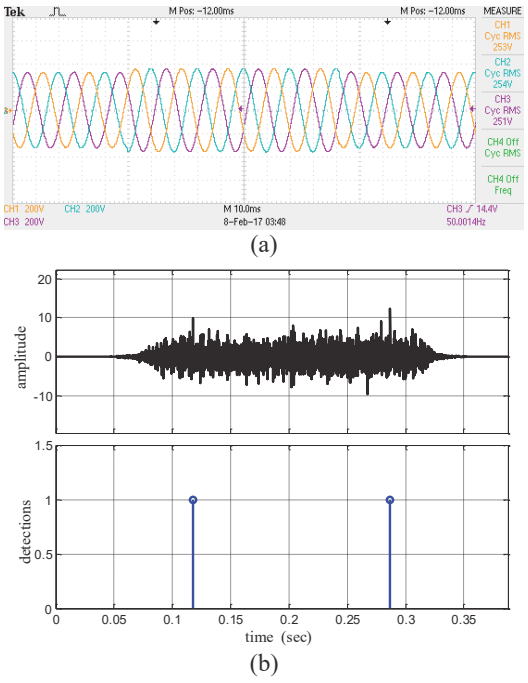

(a)

(b)

Fig. 4 Performance of the proposed system under three-phase voltage swell condition (a) captured results in oscilloscope (b) determined faulty interval.

REFERENCES

[1] A. M. Rauf and V. Khadkikar, "An enhanced voltage sag compensation scheme for dynamic voltage restorer," *IEEE Trans. Ind. Electron.*, vol. 62, no. 5, pp. 2683-2692, May 2015.

[2] S. Biricik, and H. Komurcugil, "Optimized sliding mode control to maximize existence region for single-phase dynamic voltage restorers". *IEEE Trans. on Industrial Informatics*, vol. 12, pp.1486–1497.

[3] S. Santoso, E. J. Powers, W. Mack Grady, and P. Hofmann, "Power quality assessment via wavelet transform analysis," *IEEE Trans. on Power Delivery*, vol. 11, pp. 924–930, April 1996.

[4] D. Granados-Lieberman, R.J. Romero-Troncoso, R.A. Osornio-Rios, A. Garcia-Perez, E. Cabal-Yepez, "Techniques and methodologies for power quality analysis and disturbances classification in power systems: a review." *IET Gener. Transm. Dis*., vol. 5, no. 4, pp. 519–529, 2011.

[5] S. Khokhar, A.A.B.M. Zin, A.S.B. Mokhtar, A.S.B.M. Pesaran, "A comprehensive overview on signal processing and artificial intelligence techniques applications in classification of power quality disturbances", *Renew. Sust. Energ. Rev.*, vol. 51, pp.1650–1663, 2015.

[6] A. Ferrero, M. Lazzaroni and S. Salicone, "A calibration procedure for a digital instrument for electric power quality measurement," in *IEEE Trans. on Instrumentation and Measurement*, vol. 51, no. 4, pp. 716-722, Aug. 2002.

[7] O. Poisson, P. Rioual and M. Meunier, "Detection and measurement of power quality disturbances using wavelet transform," in *IEEE Trans. on Power Delivery*, vol. 15, no. 3, pp. 1039-1044, July 2000.

[8] P.P. Vaidyanathan, "Theory of optimal orthonormal subband coders", *IEEE Trans. on Signal Process*. Vol. 46, pp. 1528–1543, 1998.

[9] P.P. Vaidyanathan, *Multirate Systems and Filter Banks*, Prentice Hall, Englewood Cliffs, 1993.

[10] J.G. McWhirter, P.D. Baxter, T. Cooper, S. Redif, J. Foster, "An EVD algorithm for para-Hermitian polynomial matrices", *IEEE Trans. on Signal Process*. vol. 55, pp. 2158–2169, May 2007.

[11] S. Redif, J.G. McWhirter, S. Weiss, "Design of FIR paraunitary filter banks for subband coding using a polynomial eigenvalue decomposition", *IEEE Trans. on Signal Process.*, vol. 59. pp. 5253–5264, Nov. 2011.

[12] M. Tohidian, H. Amindavar, A.M. Reza, "A DFT-based approximate eigenvalue and singular value decomposition of polynomial matrices", *J. Adv. Signal Process.*, vol. 1, pp. 1–16, 2013.

[13] S. Redif, S. Weiss, J.G. McWhirter, "Sequential matrix diagonalisation algorithms for polynomial EVD of parahermitian matrices", *IEEE Trans. on Signal Process*. vol. 63, pp. 81–89, Jan. 2015.

[14] S. Weiss, J. Pestana, and I. K. Proudler, "On the existence and uniqueness of the eigenvalue decomposition of a parahermitian matrix," *Trans. on Signal Process.*, vol. 66, pp. 2659–2672, Mar. 2018.

[15] S. Redif, J.G. McWhirter, P.D. Baxter, T. Cooper, "Robust broadband adaptive beamforming via polynomial eigenvalues", *IEEE/MTS OCEANS'06*, Boston, MA, Sep. 2006, pp. 1–6.

[16] S. Redif, "Fetal electrocardiogram estimation using polynomial eigenvalue decomposition, *Turk. J. Electr. Eng. Comput. Sci.*, vol. 24, pp. 2483–2497, Aug. 2014.

[17] S. Redif, S. Weiss, J.G. McWhirter, "Relevance of polynomial matrix decompositions to broadband blind signal separation", *Signal Process.*, vol. 134, pp. 76–86, 2017.

[18] S. Redif, "Convolutive blind signal separation via polynomial matrix generalized eigenvalue decomposition," *Electronic Letters*, vol. 53, pp. 87–89, Jan 2017.

[19] J.G. McWhirter and Z. Wang, "A novel insight to the SBR2 algorithm for diagonalising para-hermitian matrices," in *11th IMA Conference on Mathematics in Signal Processing*, Birmingham, U.K., Dec. 2016, pp. 1–4.

[20] N. Yoder, "PeakFinder", 2009, [Online]. Available: http://www.mathworks.com/matlabcentral/fileexchange/25500-peakfinder [Accessed: Aug. 2018].